Crystal Structure of an Aliphatic Polyoxamide Containing Methyl Side-Groups: Poly(2-methyl-1,8-octamethyleneoxamide)

Tomoyuki Nakagawa [1, 2, *], *Shuichi Maeda* [1], *Koji Nozaki* [2], *Takashi Yamamoto* [2]

[1] Organic Specialty Materials Research Laboratory, Ube Industries, Ltd., Ube, Yamaguchi 755-8633, Japan

[2] Department of Physics, Graduate School of Science and Engineering, Yamaguchi University, Yamaguchi 753-8512, Japan

*Corresponding author. Organic Specialty Materials Research Laboratory, Ube Industries, Ltd., Ube, Yamaguchi 755-8633, Japan

Tel.: +81-836-31-1746.

E-mail address: 32737u@ube-ind.co.jp (T. Nakagawa).

Abstract

Poly (2-methyl-1,8-octametyleneoxamide) (nylon-MOMD-2) was prepared from dibutyl oxalate and 2-methyl-1,8-octamethylenediamine. The chemical structure was investigated by ^{13}C nuclear magnetic resonance (^{13}C NMR). The ^{13}C NMR spectrum revealed that the methyl groups distribute among the four β-sites at random. The crystal structure and its temperature dependence were also investigated by molecular mechanics calculations, X-ray diffraction, and differential scanning calorimetry. The structure was determined to be monoclinic and a = 6.26 Å, b = 8.80 Å, c = 14.7 Å, and β = 50.7°. The torsion angle of the NH–CH_2 bonds has a skew conformation and there are the two distinct torsion angles in the crystal structure. The crystal structure of nylon-MOMD-2 has a disordered and statistical structure. The crystal structure shows no phase transition on heating until its melting point, although the unit cell expands in the a and b axis directions.

Keywords: polyoxamide, crystal structure, X-ray diffraction

1. Introduction

The crystal structures for nylons have been classified into two basic forms, namely, the α and γ forms. The even-even nylons, nylon-6,6 and nylon-6,10, crystallize in the α form[1]. The chains in the α form are in the fully extended planar zig-zag conformation. They form planar sheets of hydrogen bonded molecules. Diffraction pattern of the α form is characterized by two strong reflections at ca. 4.4 and 3.8 Å, which are related to the interchain distance within a sheet and between sheets, respectively. In the case of the even-odd, odd-even, and odd-odd nylons

have been considered to crystallize primarily in the γ form which was initially suggested by Kinoshita.[2] The γ form is characterized by a shorter chain axis caused by a 30° tilting of the amide group with respect to the chain axis. The tilting allows all hydrogen bonds to be formed. However, it has been reported that an α-like structure can also be found in several even-odd and odd-eve nylons, such as nylon-6,5[3], nylon-12,5[4], nylon-9,2[5], and nylon-5,6[6]. In these nylons, new structure models based on two hydrogen bond directions have been postulated.

The characteristic solid-solid phase transition, the so-called Brill transition[7], is sometimes observed in aliphatic nylon crystals.[8–12] Many studies on the Brill transition have been reported for various nylons[13-15] and model compounds.[13,16-18] It is considered that the mobility of the hydrocarbon chains between the amide groups increases at the Brill transition, although the hydrogen bonds between the neighboring chains still remain.[19,20] This transition is usually confirmed by X-ray diffraction, where the two strong Bragg reflections, which correspond to the chain packing of the molecules, merge into a single peak at the Brill transition. This shows that the molecular packing changes from orthorhombic to hexagonal due to disordering of the conformation of the hydrocarbon chain.

Polyoxamides (–NH–R–NH–CO–CO–) are high performance polymer materials that have a high melting point, high modulus, high chemical resistance, and low water-absorbing property. The oxamide linkage as a hydrogen bonding motif has been utilized for regular copolyamides[21] and hard segments in poly(ether amide)s.[22] Polyoxamides have amide bonds in their backbone and belong to the so-called nylon materials. The crystal structures of polyoxamides have been studied for nylon-12,2,[23, 24] nylon-10,2,[23] nylon-9,2,[5] nylon-8,2,[23] nylon-6,2,[23, 25] and nylon-4,2[26] by X-ray diffraction. Nylon-10,2, nylon-8,2, nylon-6,2,[23] and nylon-4,2 show two major reflections in their X-ray powder diffraction patterns, corresponding

to intermolecular spacings of about 4.5 and 3.7 Å. The crystal structures of nylon-12,2,[24] nylon-9,2, and nylon-6,2[25] were determined by X-ray fiber diffraction. In the crystal structure of polyoxamide with even *m* (Fig. 1), the polymer chain has an extended planar zigzag conformation. Chains arranged in the [100] direction are connected by intermolecular hydrogen bonds between neighboring chains, resulting in the formation of a molecular sheet, as shown in Fig. 2. Each neighboring sheet is displaced in the *c* direction to accommodate the oxamide groups, similar to the characteristic α-form of nylons.[27]

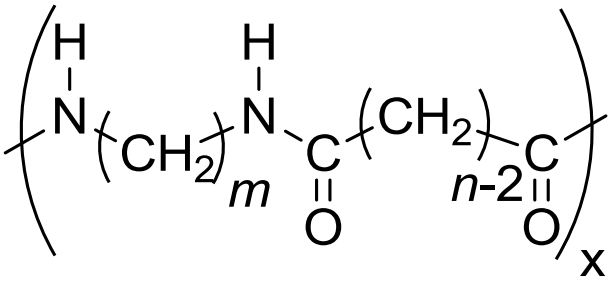

Figure 1. Chemical structure of nylon-*m*,*n*. *n* = 2 corresponds to polyoxamide.

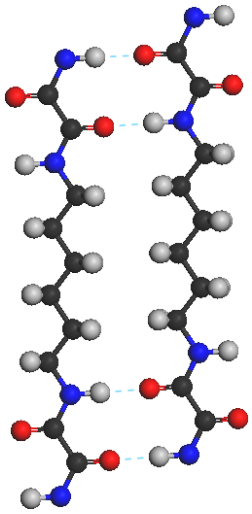

Figure 2. Typical hydrogen bonded sheet in nylon-6,2. Hydrogen bonds are indicated by dashed lines. Color code: nitrogen: blue, oxygen: red, carbon: black, and hydrogen: gray.

In the case of polyoxamides with odd *m*, only the crystal structure of nylon-9,2 has been determined,[5] which is monoclinic with space group $C\,2/c$ and lattice parameters $a = 5.45$ Å, $b = 8.7$ Å, $c = 31.8$ Å, and $\beta = 47.9°$, where the *c* direction corresponds to the chain direction. Figure 3 shows the crystal structure of nylon-9,2. The chain conformation is all-trans and the torsion angle C(O)-N(H)-C(H_2)-C(H_2) is 155°, which is compatible with hydrogen bonding between neighboring chains. Consecutive oxamide planes tilt out of the plane in opposite directions (see Fig. 3a). As a result, the crystal structure of nylon-9,2 is characterized by two types of hydrogen bonds with different directions (Fig. 3c). This crystal structure is interesting because it is different from the common γ form of crystals of odd-even nylons.[27]

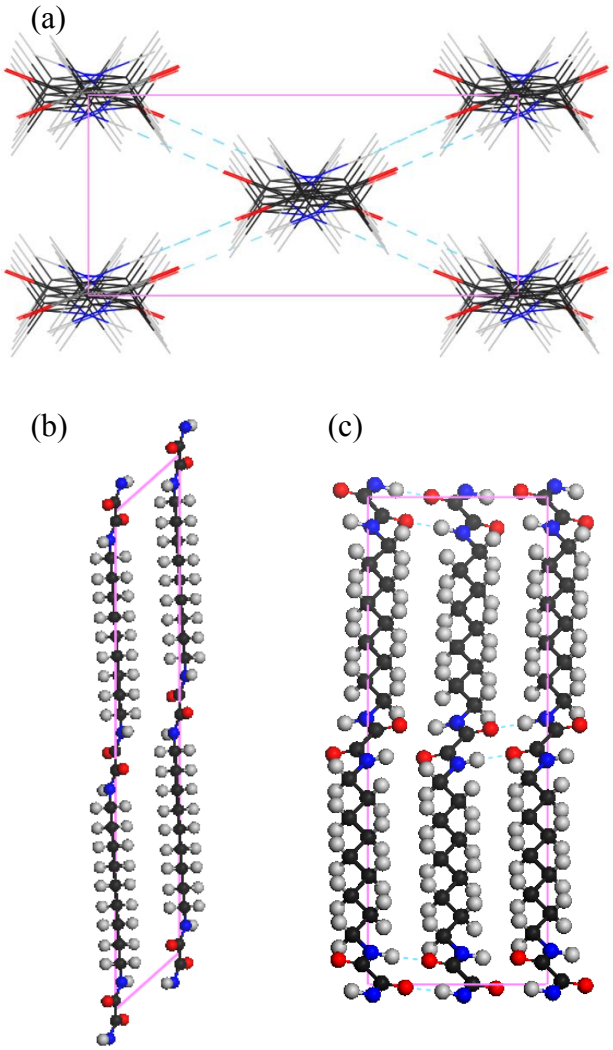

Figure 3. Schematic diagrams of the crystal structure of nylon-9,2 viewed along (a) the *c*-direction, (b) the *b*-direction, and (c) the *a*-direction. Solids pink lines indicate the unit cell and hydrogen bonds are indicated by dashed lines. Color code: nitrogen: blue; oxygen: red; carbon: black; and hydrogen: gray.

2-methyl-1,8-octamethylenediamine (MOMD) is a structural isomer of 1,9-nonamethylenediamine. MOMD contains an asymmetric carbon at the β-site and is believed to be a mixture of the two steric isomers. Nylon-MOMD-2 is a polyoxamide made from MOMD and an oxalic compound. It is expected that the methyl side-group adds to one of the four β-sites

in nylon-MOMD-2 when both ends of the diamine are randomly introduced into the polymer chain during polymerization. However, the crystal structure has not been determined. We are interested in the crystallization of nylon-MOMD-2 and the effect that methyl groups at the β-sites have on the crystal structure. In this study, the crystal structure of nylon-MOMD-2 is investigated by ^{13}C nuclear magnetic resonance, molecular mechanics calculations, and X-ray diffraction. The temperature dependence of the crystal structure is also studied.

2. Experimental

2.1. Samples

Nylon-MOMD-2 were prepared from 2-methyl-1,8-octamethylenediamine and dibutyl oxalate according to the two-step synthesis method reported by Shalaby et al.[23] Dibutyl oxalate was supplied from Ube Industries, Ltd (Ube, Japan), and MOMD was supplied by Kuraray Co Ltd (Tokyo, Japan). The intrinsic viscosity of the polymer was determined using a Ubbelohde viscometer in sulfuric acid (96% wt/wt) at 25 ± 0.1 °C. The intrinsic viscosity of nylon-MOMD-2 was 1.40 dL/g. The synthesized polymer was dried at 110 °C for 12 hours in a vacuum prior to any sample preparation or measurements.

2.2. ^{13}C Nuclear Magnetic Resonance

The chemical structures of nylon-MOMD-2 were analyzed using ^{13}C nuclear magnetic resonance (^{13}C-NMR) spectra obtained from a 5% wt/vol nylon-MOMD-2/deuterated sulfuric acid solution. The ^{13}C-NMR apparatus used here was a Bruker Biospin ADVANCE500 spectrometer operating at 125 MHz. To evaluate the position of the methyl group in the MOMD segments, the model compounds shown in Figure 4 were synthesized and then analyzed by ^{13}C-NMR under the same conditions as those for nylon-MOMD-2.

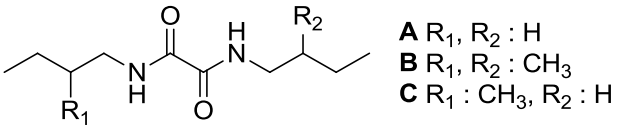

Figure 4. Three types of model compounds (A, B, and C) of nylon-MOMD-2.

2.3. Differential Scanning Calorimetry

The thermal behavior was investigated by differential scanning calorimetry (DSC) with a Perkin-Elmer Diamond DSC apparatus at a scanning rate of 10 °C/min in a helium atmosphere. A small amount of sample (1.5–2 mg) was used for the DSC measurements. The temperature of the calorimeter was calibrated using the melting temperature of an indium standard.

2.4. X-ray Diffraction

The fiber sample of nylon-MOMD-2 was prepared and then used for X-ray diffraction. A sheet with 1 mm thickness was prepared by compression molding and quenched in an ice-water bath. Then, the sheet was elongated to 200% of the initial length at 200 °C and annealed at the same temperature for an hour to give the fiber sample. X-ray fiber diffraction patterns were recorded on cylindrical films with an exposure time of 12 h at room temperature. Ni-filtered Cu-Kα radiation (λ = 1.542 Å) from an X-ray generator (RIGAKU RAD IA) operating at 35 kV and 20 mA was used. The camera diameter (R = 35.01 mm) was calibrated from the Bragg peaks of Si standard powder.

Integrated intensities of a few relatively strong reflections were collected to determine the molecular arrangement within the unit cell. The integrated intensities of the Bragg peaks were determined by peak separation of the X-ray powder diffraction pattern of the non-oriented isotropic sample. The sample was prepared by melt-crystallization at 215 °C for 17 h in a glass

tube with a diameter of 5 mm. X-ray powder diffraction patterns were recorded for 30 minutes using a Bulker AXS DIP220 with a two-dimensional detector (imaging plate system). A monochromatized Cu-Kα beam (40 kV, 250 mA) was transmitted through the sample. The intensity-2θ profiles were obtained from the 2D X-ray diffraction profiles. The software Origin 8.5.1 (LightStone Corp.; Tokyo, Japan) was used for the peak separation of the Bragg peaks. Deconvolution of the powder diffraction patterns into Bragg peaks, amorphous halo profiles, and background was performed. Bragg peaks were fitted to the Lorenz function. The X-ray scattering profile of the quenched film of nylon-MOMD-2 was used as the amorphous halo profiles.

X-ray diffraction patterns at high temperature were also collected to investigate the temperature dependence of the crystal structure of nylon-MOMD-2. The sample was held in the sample holder of a metal-block furnace. The temperature of the sample was measured by a thermocouple in contact with the sample and was controlled with a PID controller within ±0.1 °C. The Bulker AXS DIP220 system was also used. After an X-ray diffraction pattern was recorded on the imaging plate with an exposure time of 5 min at a desired temperature, the sample was heated to the next temperature. This measurement process was repeated under heating until the sample melted. After melting of the sample, measurements were repeated by cooling to room temperature.

2.5. Molecular mechanics calculations

Molecular mechanics (MM) calculations were carried out using Forcite in Materials Studio 6.0 (Accelrys, Inc.; San Diego, CA, USA) to determine the molecular configuration and arrangement in the unit cell. The Universal[28-30] force field was used for the calculations.

3. Results and Discussion

3.1. Chemical Structure of Nylon-MOMD-2

Figure 5 shows the ^{13}C NMR spectrum of nylon-MOMD-2. Peaks a–i in Fig. 5b are assigned to the signals from the carbon atoms represented by a–i in Fig. 5a. The peaks around 158 ppm can be attributed to the carbonyl carbon atoms in the oxamide groups. The chemical shift of the carbonyl carbon atom is sensitive to the chemical environment of the oxamide group.[31] In the case of nylon-MOMD-2, three different chemical environments of the oxamide group are possible (i) without methyl groups at the β-sites, (ii) with two methyl groups at both of the β-sites, and (iii) with one methyl group at one of the four β-sites. The chemical environments (i)–(iii) represent the model molecules A–C in Fig. 4, respectively. Hence, the NMR spectrum of the carbonyl carbon atom is used to analyze the distribution of the methyl groups in the nylon-MOMD-2 molecules.

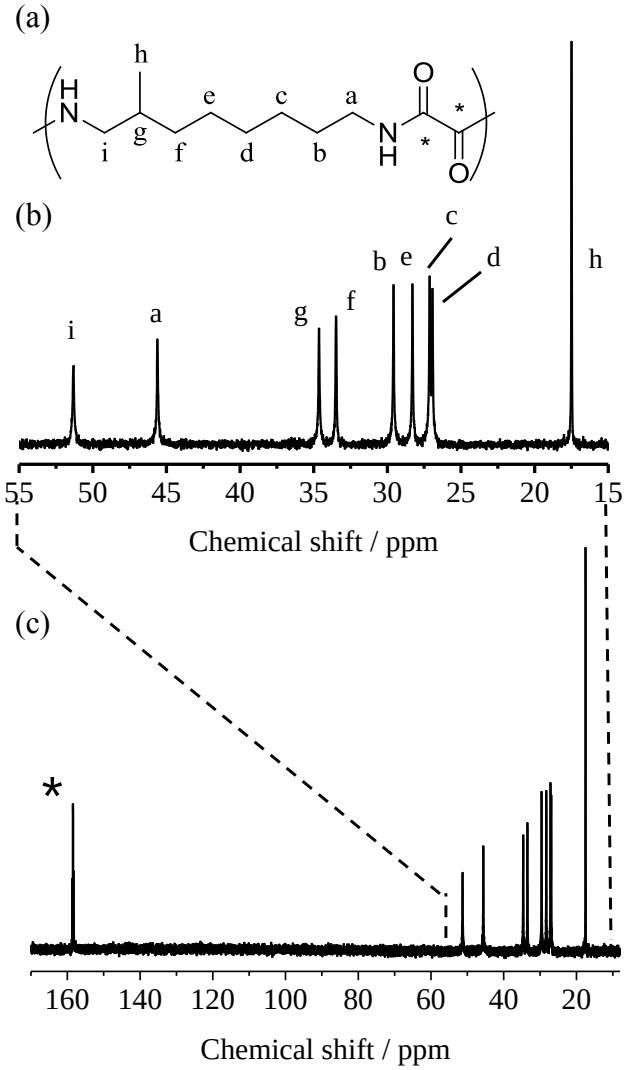

Figure 5. ^{13}C NMR spectrum of nylon-MOMD-2. (a) (b) The expanded spectrum from 15 ppm to 55 ppm. (c) The overall spectrum from 15 ppm to 170 ppm. Peaks a–i are assigned to the signals from the carbon atoms represented by a–i in (a).

Figure 6(a) shows the ^{13}C NMR spectrum of the carbonyl carbon atom in nylon-MOMD-2. ^{13}C NMR spectra of the model compounds A, B, C, and a mixture of the model compounds A, B, and C with the molar ratio of 1:1:2 are also shown in Fig. 6(b), (c), (d), and (e), respectively. The NMR spectrum of nylon-MOMD-2 in Fig. 6(a) has three carbonyl carbon peaks at 158.2

(peak a'), 158.4 (peak c'), and 158.6ppm (peak b'). From the comparison with the NMR spectrum of nylon-MOMD-2 and those of the model compounds, the peaks at 158.2, 158.6, and 158.4ppm are considered to be the signal of the carbonyl carbon atom of the oxamide group in the same chemical environments as in the model compounds A, B, and C (peak a in Fig. 6(b), peak b in Fig. 6(c), and peaks c_1 and c_2 in Fig. 6(d), respectively). It should be noted that chemical shifts of the peaks a', b' and c' of the nylon-MOMD-2 are slightly larger than those of the peaks a, b, c_1, and c_2 of the model compounds. Furthermore, the peak c' of nylon-MOMD-2 is a singlet, although for the model compound C the peak clearly splits into the two peaks c_1 and c_2. These are considered to be due to the difference in chain length of the aliphatic chain in nylon-MOMD-2 and the model compounds. Thus, we conclude that the NMR spectrum of the carbonyl carbon in the nylon-MOMD-2 molecules is essentially the same as that of the mixture of the model compounds. The intensity ratio of a':c':b' in Fig. 6(a) is approximately 1:2:1, being consistent with the intensity ratio of a : $c_1 + c_2$: b in Fig. 6(e). The ratio is also equal to the intensity ratio of the polymer in which the three oxamide bonds statistically produce. Therefore, the methyl groups are randomly added at the β-sites of the oxamide bond of the nylon-MOMD-2 molecules.

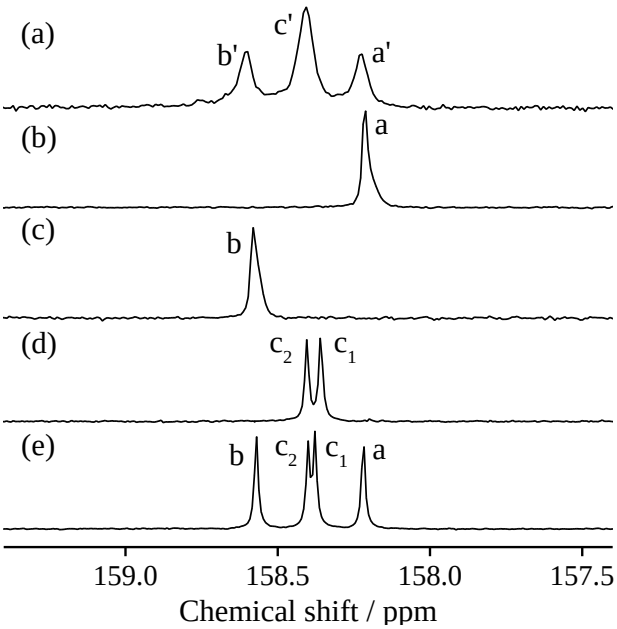

Figure 6. ^{13}C NMR spectra of carbonyl carbon atoms in (a) nylon-MOMD-2, (b) model compound A, (c) model compound B, (d) model compound C, and (e) a mixture of model compounds A, B, and C with the molar ratio of 1:1:2.

3.2. Crystal Structure of nylon-MOMD-2

Figure 7 shows the X-ray diffraction pattern of an oriented fiber sample of nylon-MOMD-2 at room temperature. The positions of the observed Bragg reflections were converted to the corresponding reciprocal coordinates, and a monoclinic unit cell was chosen as the corresponding reciprocal positions of all Bragg reflections to agree with its reciprocal lattice points. The initial values of the unit cell parameters were determined from the positions of the observed Bragg reflections and optimized by least squares method. The *R* factor is 0.012, where

$$R = \frac{\sum |\theta_{cal} - \theta_{obs}|}{\sum \theta_{cal}} \quad . \qquad (1)$$

θ_{cal} and θ_{obs} are the calculated and observed scattering angles, respectively. The unit cell parameters finally obtained are listed in Table 1. Indices of the observed Bragg reflections are listed in Table 2, as well as observed (d_{obs}s) and calculated *d*-spacings (d_{cal}s). There is good agreement between the d_{cal}s and d_{obs}s values. Only reflections with $h + k$ = even are observed for the *hkl* reflections. This indicates that the crystal lattice has *C*-centered symmetry. Therefore, possible space groups of the crystal are *C*2, *Cm*, and *C*2/*m*. The specious space group is *C*2/*m* when the molecular configuration and the statistical structure of nylon-MOMD-2 are taken into account, as will be discussed below.

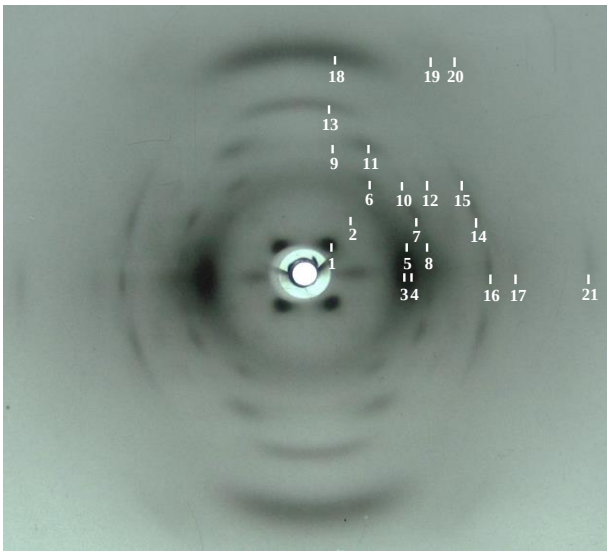

Figure 7. X-ray diffraction pattern of the oriented fiber of nylon-MOMD-2. Twenty one major Bragg reflections were observed and numbered beginning at the reflection at the lowest scattering angle.

Table 1 Unit cell parameters of the nylon-MOMD-2 crystal.

a (Å)	*b* (Å)	*c* (Å)	β (°)
6.26±0.06	8.80±0.08	14.74±0.15	50.7±0.5

Table 2 Observed and calculated *d*-spacings of the nylon-MOMD-2 crystal. Abbreviations denote intensities: vs: very strong, s: strong, m: medium, w: weak, and vw: very weak.

No	Index	Calcd. *d*(Å)	Obsd. *d*(Å)
1	001	11.51	11.64vs
2	002	5.76	5.85 w
3	020	4.48	4.49 vs
4	110	4.24	4.26 vs
5	021	4.17	4.14 w
6	003	3.84	3.86 s
7	022	3.54	3.54 s
8	$\bar{1}11$	3.42	3.44 w
9	114	3.41	3.41 vw
10	203	3.09	3.11 vw
11	204	2.98	3.09 s
12	023	2.91	2.87 vw
13	205	2.72	2.73 m
14	222	2.48	2.47 s
15	024	2.42	2.41 vw
16	200	2.41	2.43 s
17	116	2.28	2.21 s
18	220	2.12	2.13 vw
19	316	1.94	1.97 vw
20	136	1.85	1.84 w
21	240	1.64	1.60 w

The molecular configuration of nylon-MOMD-2 in the crystalline phase was predicted using MM calculations. Figure 8 shows molecular models of nylon-MOMD-2 used for the MM calculations. The models are composed of two MOMD chains connected by an oxamide bond and have finite length, and the ends of each MOMD chain are amine-terminated oxamide bonds. Since ^{13}C NMR analysis showed that the methyl groups are randomly distributed among the four β-sites in nylon-MOMD-2, we built four molecular models with different numbers and positions of the methyl groups (D–G in Fig. 8). MM calculations were performed to determine the molecular conformation with the minimum potential energy. The results obtained for each model are summarized in Table 3. In all cases (D–G in Fig.8), the torsion angles (ω_1, ω_2 and ω_3) in the oxamide group prefer the trans conformation. The two $–CH_2–NH–$ dihedral angles (Φ_1 and Φ_1') in the oxamide group with a methyl group at neighboring β-sites are approximately 120° (*skew*) except Φ_1' of model G, while Φ_1 and Φ_1' without a methyl group at neighboring β-sites are about 180° (*trans*). Alemán et al. studied the effect of the methyl side group in aliphatic diamine on the conformation of polymethylene segment of polyamide by ab initio methods.[32] They found that the two $–CH_2–NH–$ dihedral angles in a model compound with a β-methyl group prefer the skew conformation. In the case of models F and G in Fig.8, a methyl group is added at each β-site on both sides of the oxamide group. The two model molecules are different in configuration. Therefore, the minimum energy conformations of models F and G are different. For model F in Fig. 8, the two dihedral angles Φ_1 and Φ_1' are approximately −120° (*skew*−) and +120° (*skew*+), respectively, according to the result of the MM calculations in Table 3. On the other hand, for model G Φ_1' is −166.4°, which is close to the trans conformation. In the latter case, the molecular chain bends in the actual polymer chain, and cannot be arranged in the crystalline region. Considering the long-chained molecule of nylon-MOMD-2, the molecule should have an

almost fully extended conformation in the crystalline state. When two –CH_2–NH– dihedral angles (Φ_1 and Φ_1') are 180° (*trans*), the molecular chain has the fully extended conformation. In this case, however, the repeating unit of the chain is too long for the determined lattice constant *c*, and cannot be fitted to the unit cell.

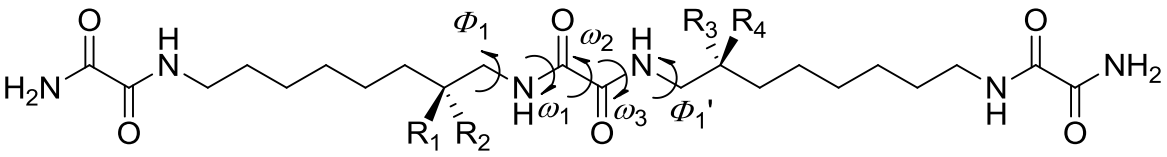

D R_1, R_2, R_3, R_4 : H, **E** R_1 : CH_3, R_2, R_3, R_4 : H,
F R_1 : CH_3, R_2 : H, R_3 : CH_3, R_4 : H, **G** R_1 : CH_3, R_2, R_3 : H, R_4 : CH_3

Figure 8. Four types of model compounds (D–G) of nylon-MOMD-2 used for the molecular mechanics calculations.

Table 3 Torsion angles obtained from the molecular mechanics calculations of model compounds (D–G).

	Torsion angle (^{o})				
	Φ_1	ω_1	ω_2	ω_3	Φ'_1
D	180.0	180.0	180.0	180.0	180.0
E	-117.5	-179.4	179.9	180.0	180.0
F	-117.5	-179.4	180.0	179.4	117.6
G	-117.8	-179.6	177.9	-177.6	-166.4

Finally, we assumed that the two –CH_2–NH– dihedral angles Φ_1 and Φ_1' were −120° (*skew*−) and +120° (*skew*+) and the three torsion angles ω_1, ω_2 and ω_3 were 180° (*trans*), similar to those of model F. The assumed molecular conformation of nylon-MOMD-2 in the crystalline

state is shown in Fig. 9. If a segment of the nylon-MOMD-2 chain has the same configuration as models D, E or G, the segment is expected to have a similar conformation to the one shown in Fig. 9, or it may be rejected from the crystal region during crystallization.

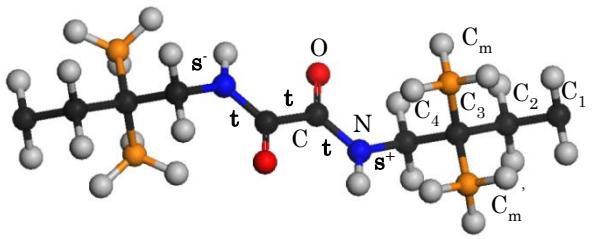

Figure 9. Conformation of the nylon-MOMD-2 molecule in the crystalline state. Methyl groups are added at the four β-sites to represent the statistical structure of the nylon-MOMD-2 crystal. Two $-CH_2-$ NH– dihedral angles are *skew*− (**s**$^-$) and *skew*+ (**s**$^+$) and three torsion angles in the oxamide group are *trans* (**t**). Color code: nitrogen: blue, oxygen: red, carbon of the backbone: black, carbon at β-site: orange, and hydrogen: gray.

In the crystalline state, the nylon-MOMD-2 molecules are expected to form a hydrogen bonding network with neighboring chains. The crystal structure is predicted by packing the molecules with the assumed conformation in the unit cell, to form the hydrogen bonding network shown in Fig. 10. The atomic coordinates of the carbon, nitrogen, and oxygen atoms of the asymmetric structural unit are listed in Table 4. The ^{13}C NMR results indicate that the methyl groups are randomly added to the β-sites in nylon-MOMD-2. Moreover, the molecules take one of the two conformations that are related by mirror symmetry. As a result, the hydrogen bond in the *ab* projection of the nylon-MOMD-2 crystal is along either the [110] or [$1\bar{1}0$] direction. This causes the *c* dimension of nylon-MOMD-2 (14.7 Å) to decrease to about a half of the *c* dimension of nylon-9,2 (31.8 Å). In other words, the parameter *c* of the unit cell of nylon-

MOMD-2 corresponds to one repeat length, while the parameter *c* of the unit cell of nylon-9,2 corresponds to two repeat lengths. Hence, the crystal structure of nylon-MOMD-2 is more disordered than that of nylon-9,2.

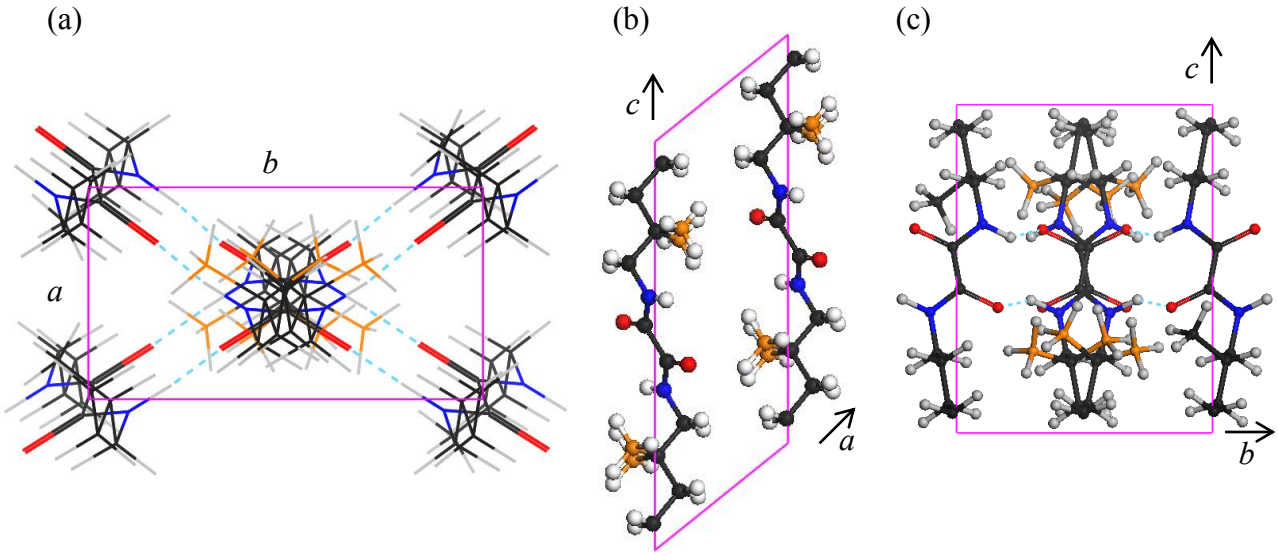

Figure 10. Schematic diagrams of the crystal structure of MOMD-2 viewed along (a) the *c*-direction, (b) the *b*-direction, and (c) the *a*-direction. Note that two types of molecules are drawn at the center of (a) and (c) to describe the statistical structure. Solids pink lines show the unit cell and hydrogen bonds are indicated by dashed pale blue line. Color code: nitrogen: blue, oxygen: red, carbon of the backbone: black, carbon at β-site: orange, and hydrogen: gray.

Table 4 Atomic coordinates of the asymmetric structural unit of the nylon-MOMD-2 crystal. C_m and C_m' are the carbon atoms of the methyl groups at the β-sites. The occupation factors are selected by taking into account the statistical structure in the nylon-MOMD-2 crystal.

Atom	Coordinates of the atoms			f_o[a]
	x	y	z	
C_1	0.0356	0.0035	0.4367	0.5
C_2	-0.1674	-0.0139	0.4130	0.5
C_3	-0.0090	-0.0483	0.2829	0.5
C_4	-0.2132	-0.0649	0.2600	0.5
C_m	0.1798	0.0806	0.2022	0.25
C_m'	0.1490	-0.1956	0.2510	0.25
N	-0.0630	-0.0986	0.0959	0.5
C	-0.0789	0.0163	0.0639	0.5
O	-0.2505	0.1636	0.1180	0.5

[a]Occupation factor.

To evaluate the predicted crystal structure of nylon-MOMD-2, the intensities of the Bragg reflections were calculated from the model structure and compared with the observed intensities. For the following reason, quantitative analysis of the integrated intensities of the Bragg reflections was performed by using X-ray powder diffraction pattern of an isotropic specimen. Calculating an integrated intensity of a Bragg reflection from a X-ray diffraction pattern usually requires various data corrections. The fiber sample used here may have preferred orientation in a plane perpendicular to the fiber axis. In such case, complicate data corrections should be applied to get the integrated intensity of a Bragg reflection in consideration of the preferred orientation.

The intensity of a Bragg reflection is given by

$$I(hkl) = C|F(hkl)|^2 \exp(-2M), \qquad (2)$$

where $F(hkl)$ is the structure factor and C is the product of the Lorentz factor, polarization factor and multiplicity of the Bragg reflection. The factor $\exp(-2M)$ is Debye-Waller factor, and M is given by

$$M = 8\pi^2 < u^2 > \left(\frac{\sin\theta}{\lambda}\right)^2 = B\left(\frac{\sin\theta}{\lambda}\right)^2, \qquad (3)$$

where λ, θ, and $<u^2>$ are the wavelength of X-rays, half of the scattering angle 2θ, and the mean square displacement of the molecule, respectively. $B = 8\pi^2<u^2>$ is the temperature factor. Figure 11 shows the peak separation procedure of the whole XRD profile into the individual Bragg reflection peaks. In this peak separation process, the Bragg peak was fitted to the Lorentzian curve. By comparing the synthesized profile of the individual Bragg reflection peaks, the amorphous halo, and the background to the observed XRD profile, the profiles of the Bragg reflection peaks were optimized. The amorphous halo profile used here was measured using quenched nylon-MOMD-2 film. The observed intensities $I_o(hkl)$ were obtained by integration the Bragg reflection peaks optimized above. The integrated intensity of the Bragg peak at $2\theta = 25.70^\circ$ and that at $2\theta = 37.64^\circ$ were treated as the sum of $I_o(022)$, $I_o(\bar{1}11)$ and $I_o(114)$, and the sum of $I_o(222)$, $I_o(024)$ and $I_o(200)$, respectively.

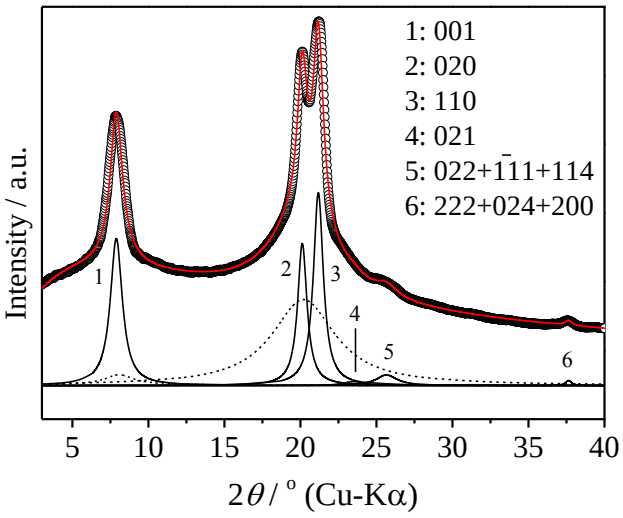

Figure 11. Peak separation process of the X-ray diffraction profiles of the isotropic specimen of the nylon-MOMD-2 crystal. Separated Bragg peaks are shown as solid lines and amorphous peaks are shown as dashed lines.

The calculated intensities $I_c(hkl)$ were obtained from the equation

$$I_c(hkl) = C\left|F_{\text{mode}}(hkl)\right|^2 \exp(-2M), \qquad (4)$$

where F_{model} is an ideal structure factor for the model structure shown in Fig. 10, and was calculated using the atomic coordinates in Table 4. We estimated the value of the B factor in eq. (3) as 30 Å^2.

The $I_o(hkl)$ and $I_c(hkl)$ values are listed in Table 5, where all of the values are normalized to $I_o(110)$ and $I_c(110)$, respectively. The calculated intensities approximately agree with the observed values except for the 222, 024, and 200 reflections. In this work, we cannot optimize the structural model because a number of the Bragg reflections is quite small compared to a number of structural parameters. Besides, we assumed the isotropic temperature factor. However, the actual molecules will undergo anisotropic fluctuations. This is a possible reason for the

difference between the calculated and observed structure factors of the 222, 024, and 200 Bragg reflections. Thus, we conclude that the crystal structure predicted here is reasonable.

Table 5 Observed and calculated structure factors of nylon-MOMD-2.

Peak No.	2θ / °	Index	I_o	I_c
1	7.90	001	57.9	47.9
2	20.10	020	58.6	40.6
3	21.20	110	100	100
4	23.00	021	4.65	4.90
5	25.70	022	5.57	0.57
		$\bar{1}11$		1.90
		114		1.08
6	37.64	222	1.16	0.06
		024		0.01
		200		0.01

3.3. Temperature variation of the crystal structure

Figure 12 shows the DSC thermograms of nylon-MOMD-2. The initial sample was crystallized from the melt and subsequently annealed at 200 °C. On heating, three endothermic peaks at 214 °C (12.5 J/g), 226 °C (13.6 J/g), and 235 °C (33.9 J/g) are observed (Fig.12 (a)). The endothermic peak at 231 °C upon heating is considered to be the melting peak. The small endothermic peaks at 214 and 226 °C are observed in the DSC heating curve. The endothermic heats correspond to 37% and 40% of the heat of fusion at 231 °C, respectively. It was reported that the endothermic heat at the Brill transition of nylon-6,6, which has a similar

methylene/amide ratio to nylon-MOMD-2, is about 16% of its heat of fusion.[33] The amount of the small endothermic heats at 214 °C and 226 °C of nylon-MOMD-2 are clearly different from that of the Brill transition. In the case of crystalline polymers, partial melting and reorganization often occurs upon heating.[34,35] Therefore, the small peaks are probably due to the melting of small crystallites. When the sample is heated up to temperatures above 203 °C, 222 °C, and 228 °C , no exothermic peaks are observed in the successive cooling runs (Fig.12 (a'), (b'), and (c'), respectively). Although small exothermic-like anomalies are found in the cooling thermograms in Figs. 12 (b'), (c') and (d'), these peaks are not caused by phase transitions. These anomalies probably originate from the recovery of the thermal stability of the DSC furnace from the switching between the heating and the cooling. On cooling the molten sample, two exothermic peaks at 209 and 177 °C are observed (Fig.12 (a')). These peaks are considered to be the crystallization peaks. The sharp exothermic peak at 209 °C is due to main crystallization, while the broad peak at 177 °C may be attributed to the secondary crystallization.

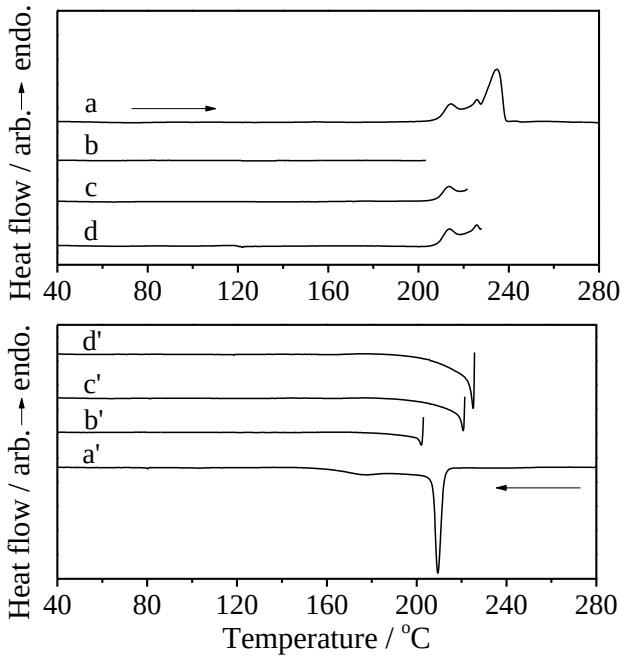

Figure 12. DSC thermograms of nylon-MOMD-2. Upper and under thermograms correspond to the heating and successive cooling processes, respectively.

Figure 13 shows the temperature dependence of the *d*-spacings of the (020) and (110) planes (d_{020} and d_{110}) of nylon-MOMD-2. The initial sample was crystallized from the melt and subsequently annealed at 200 °C. The change in the *d*-spacing is reversible with regards to the heating and cooling processes. Both the d_{020} and d_{110} values continuously increase with increasing temperature due to thermal expansion. These variations of the packing of the side-chains were clearly different from that of the Brill transition. Franco and coworkers have reported the temperature variation of the crystal structure of nylon-9,2[5]. The two strong reflections (020 and 110) were observed at room temperature at 4.34 and 3.68 Å. While the spacing of the first diffraction signal remained practically constant, the second one increased with temperature until a maximum spacing of ca. 4.05 Å, reached at 215 °C (ca. 30 °C before melting). They thought that the observed change on lattice parameters with temperature was

mainly caused by an enhanced mobility of methylenes. This result indicates that the orthorhombic side packing of the chains gets close to hexagonal packing. The Brill transition is generally accompanied by a change in the packing of the side-chains from orthorhombic to hexagonal. Therefore, the temperature variation behavior of the packing of the side-chains may be a precursor to the Brill transition. However, the nylon-9,2 crystal did not reach the Brill transition until melting. In the case of nylon-MOMD-2, the crystal structure is disordered, and the conformation of the alkyl chains may be disordered due to their statistical structures. In this situation, the packing of the side-chains is originally close to that observed in the high-temperature phase above the Brill transition temperature, and only thermal expansion of the lattice may be observed. Hence, the Brill transition no longer occurs in the nylon-MOMD-2 crystal.

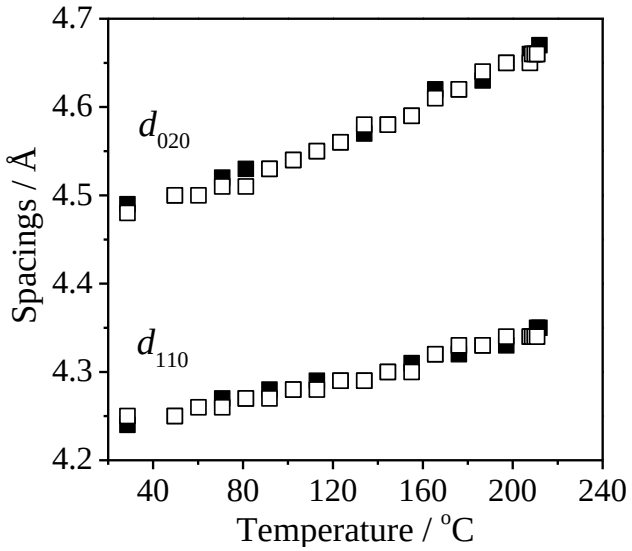

Figure 13. Temperature variations of *d*-spacings of nylon-MOMD-2 during the heating (black square) and cooling (white square) processes.

We have investigated the crystal structure of nylon-MOMD-2, and the temperature variation of the crystal structure by ^{13}C NMR, molecular mechanics, X-ray diffraction, and DSC. The major results are summarized as follows:

The nylon-MOMD-2 crystal has a monoclinic unit cell with a = 6.26 Å, b = 8.80 Å, c = 14.7 Å, and β = 50.7°. The crystal structure of nylon-MOMD-2 is a disordered and statistical structure. The methyl groups are randomly added to one of the four possible β-sites in the molecular chain, and the torsion angle of the NH-CH_2 bonds take a skew+ or skew− conformation to avoid the steric hindrance of the methyl groups added at the β-sites. The molecules have one of two conformations that are related by mirror symmetry. As a result, the hydrogen bonding in the *ab* projection is either along the [110] or [1$\bar{1}$0] direction. No phase transition is observed for the nylon-MOMD-2 crystal upon heating until its melting temperature.

Acknowledgements

The authors are particularly indebted to Dr. Naiki of Ube Industries, Ltd. for his help in preparation of this article. The authors also thank M. Gondo of Yamaguchi University for his help in obtaining the fiber pattern reported here.

References

(1) Bunn CW, Garner EV. Proc R Soc London Ser A 1947;189:39-68.

(2) Kinoshita Y. Makromol Chem 1959;33:1-20.

(3) Navarro E, Franco L, Subirana JA, Puiggalí J. Macromolecules 1995;28:8742-50.

(4) Navarro E, Subirana JA, Puiggalí J. Polymer 1997;38:3429-32.

(5) Puiggalí J, Franco L, Alemán C, Subirana JA. Macromolecules 1998;31:3912-24.

(6) Puiggalí J, Franco L, Alemán C, Subirana JA. Macromolecules 1998;31:8540-8.

(7) Brill R. J Prakt Chem 1942;161:49.

(8) Jones NA, Atkins EDT, Hill MJ, Cooper SJ, Franco L. Macromolecules 1996;29:6011-18.

(9) Jones NA, Atkins EDT, Hill MJ. J Polym Sci Part B Polym Phys 2000;38:1209-21.

(10) Jones NA, Atkins EDT, Hill MJ. Macromolecules 2000;33:2642-50.

(11) Jones NA, Atkins EDT, Hill MJ, Cooper SJ, Franco L. Polymer 1997;38:2689-99.

(12) Jones NA, Cooper SJ, Atkins EDT, Hill MJ, Franco L. J Polym Sci, Polym Phys 1997;35:675-88.

(13) Yoshioka Y, Tashiro K. Polymer 2003;44:7007-19.

(14) Huang Y, Li WH, Yan DY. Eur Polym J 2003;39:1133–40.

(15) Cui XW, Yan DY. Eur Polym J 2005;41:863–70.

(16) Harings JAW, Yao Y, Graf R, Van Asselen O, Broos R, Rastogi S. Langmuir 2009;25:7652-66.

(17) Harings JAW, Van Asselen O, Graf R, Broos R, Rastogi S. Cryst Growth Des 2008;8:2469-77.

(18) Harings JAW, Van Asselen O, Graf R, Broos R, Rastogi S. Cryst Growth Des 2008;9:3323-34.

(19) Tashiro K, Yoshioka Y. Polymer 2004;45:6349-55.

(20) Yoshioka Y, Tashiro K, Ramesh C. Polymer 2003;44:6407-17.

(21) Tirrell D, Vogl O J. Polym Sci Polym Chem Ed 1977;15:1889-903.

(22) Sijbrandi NJ, Kimenai AJ, Mes EPC, Broos R, Bar G, Rosenthal M, Odarchenko Y, Ivanov DA, Dijkstra PJ, Feijen J. Macromolecules 2012;45:3948-3961.

(23) Shalaby SW, Pearce EM, Fredericks RJ, Turi EA. J Polym Sci Polym Phys Ed 1973;11:1-14.

(24) Casas MT, Armelin E, Alemán C, Puiggalí J. Macromolecules 2002;35:8781-87.

(25) Chatani Y, Ueda Y, Tadokoro H, Deits W, Vogl O. Macromolecules 1978;11:636-8.

(26) Gaymans RJ, Venkatraman VS, Schuijer SJ. Polym Sci Polym Chem Ed 1984;22:1373-82.

(27) Xenopoulos A, Clark ES. In: Kohan MI, editor. Nylonplastics handbook, Chap 5. Munich, Vienna and New York: Hanser Publishers; 1995. p. 108-37.

(28) Rappé AK, Casewit CJ, Colwell KS, Goddard WA, Skiff WM. J Am Chem Soc 1992;114:10024-35.

(29) Casewit CJ, Colwell KS, Rappé AK. J Am Chem Soc 1992;114:10035-46.

(30) Casewit CJ, Colwell KS, Rappé AK. J Am Chem Soc 1992;114:10046-53.

(31) Abajo JD, Kricheldorf HR. J Macromol Sci Chem 1984:A21(4) 411-426.

(32) Alemán C, Puiggalí J. Macromol Theory Simul 2000;9:242-248.

(33) Howard WS, Glover AJ. J Polym Sci Polym Phys Ed 1981;19:467-77.

(34) Wunderlich B. Macromolecular Physics; Academic Press: New York, 1973.

(35) Stein SL, Paul JP. European Polym J 2007;43:1933–51.